Biochimica et Biophysica Acta 1817 (2012) 287–297

Contents lists available at SciVerse ScienceDirect

Biochimica et Biophysica Acta

journal homepage: www.elsevier.com/locate/bbabio

Two functional sites of phosphatidylglycerol for regulation of reaction of plastoquinone Q_B in photosystem II

Shigeru Itoh [a,*,1], Takashi Kozuki [a], Koji Nishida [a], Yoshimasa Fukushima [a,1], Hisanori Yamakawa [a], Ildikó Domonkos [b], Hajnalka Laczkó-Dobos [b], Mihály Kis [b], Bettina Ughy [b], Zoltán Gombos [b,**]

[a] Nagoya University, Graduate School of Science, Division of Material Science (Physics), Chikusa, Nagoya, Aichi 464-8602, Japan
[b] Institute of Plant Biology, Biological Research Centre, Hungarian Academy of Sciences, H-6701 Szeged, Hungary

ARTICLE INFO

Article history:
Received 11 April 2011
Received in revised form 7 October 2011
Accepted 11 October 2011
Available online 18 October 2011

Keywords:
Chlorophyll fluorescence
Lipid
Oxygen evolution
Phosphatidylglycerol
Photosystem II assembly
Q_B plastoquinone

ABSTRACT

Functional roles of an anionic lipid phosphatidylglycerol (PG) were studied in *pgsA*-gene-inactivated and *cdsA*-gene-inactivated/phycobilisome-less mutant cells of a cyanobacterium *Synechocystis* sp. PCC 6803, which can grow only in PG-supplemented media. 1) A few days of PG depletion suppressed oxygen evolution of mutant cells supported by *p*-benzoquinone (BQ). The suppression was recovered slowly in a week after PG re-addition. Measurements of fluorescence yield indicated the enhanced sensitivity of Q_B to the inactivation by BQ. It is assumed that the loss of low-affinity PG (PG_L) enhances the affinity for BQ that inactivates Q_B. 2) Oxygen evolution without BQ, supported by the endogenous electron acceptors, was slowly suppressed due to the direct inactivation of Q_B during 10 days of PG depletion, and was recovered rapidly within 10 h upon the PG re-addition. It is concluded that the loss of high-affinity PG (PG_H) displaces Q_B directly. 3) Electron microscopy images of PG-depleted cells showed the specific suppression of division of mutant cells, which had developed thylakoid membranes attaching phycobilisomes (PBS). 4) Although the PG-depletion for 14 days decreased the chlorophyll/PBS ratio to about 1/4, florescence spectra/lifetimes were not modified indicating the flexible energy transfer from PBS to different numbers of PSII. Longer PG-depletion enhanced allophycocyanin fluorescence at 683 nm with a long 1.2 ns lifetime indicating the suppression of energy transfer from PBS to PSII. 5) Action sites of PG_H, PG_L and other PG molecules on PSII structure are discussed.

1. Introduction

The negatively charged lipid phosphatidylglycerol (PG) is a ubiquitous component of thylakoid membranes of cyanobacterial and plant chloroplasts and constitutes 5–10% of total lipids [1]. The loss of PG affects the structure of thylakoid membranes [2,3], and damages the function of both PS I and PS II reaction centers (RC) [4–7]. In the structure of photosystem I reaction center complex (PS I RC) of *Thermosynechococcus elongatus*, the X-ray crystallography study [8] revealed four lipid molecules on the reducing side of the PsaA and PsaB polypeptides. Two PG molecules are at the peripheral moiety and one PG and one monogalactosyldiacylglycerol (MGDG) are located near the electron acceptor phylloquinone molecules (A_1 and A_1') [8]. The amount of PS I was decreased in the PG-depleted mutant cells of *Synechocystis* sp. PCC6803 [4]. Especially PSI trimers were decreased significantly in parallel with the decrease of PsaL subunit suggesting that PG is located at the center of PS I trimers associated with the PsaL subunits too [4].

X-ray crystallography studies of PS II RC of *Thermosynechococcus elongatus* [9,10] have indicated multiple lipid molecules. Two PG molecules are identified in a 3.0 Å PSII structure [10]. One PG molecule (denoted as PG_2 in Fig. 1) was located between the D1 and CP43 proteins at the postulated pathway for the exchange of Q_B quinone. Biochemical assays, on the other hand, indicated associations of 6–7 molecules of PG in the purified PS II RC of *Thermosynechococcus elongatus* and plant PS II RCs [11] indicating that some PSII-bound PG molecules were not identified yet in the structure. A recent 1.9 Å structure of PSII of this organism [12] identified these two PG too and revealed another 3 PG (altogether 5 PG) with other 6 monogalactosyldiacylglycerol (MGDG), 5 digalactosyldiacylglycerol (DGDG) and 4 sulfoquinovosyldiacylglycerol (SQDG) molecules as

Abbreviations: *APC*, allophycocyanin; *BQ*, *p*-benzoquinone; Chl, chlorophyll; $D_{(BQ)}$ and $D_{2(int)}$, decay of fluorescence yield measured with and without BQ; DCMU, 3-(3′,4′-dichlorophenyl)-1,1-dimethylurea; DGDG, digalactosyldiacylglycerol; MGDG, monogalactosyldiacylglycerol; $O_{2(BQ)}$ and $O_{2(int)}$, oxygen evolution activity with and without BQ, respectively; PAM, pulse amplidue modulation; PC, phycocyanin; PG, phosphatidylglycerol; PG_H and PG_L, PG bound to the high- and low-affinity sites that regulate the Q_B function, respectively; PG1-5, PG molecules identified in the structure of PS II; PS, photosystem; Q_A and Q_B, first and second electron acceptor plastoquinoneof PSII; RC, reaction center; SQDG, sulfoquinovosyldiacyglycerol; WT, wild type

* Corresponding author. Tel./fax: +81 52 789 4739.
** Corresponding author.
E-mail addresses: itoh@bio.phys.nagoya-u.ac.jp (S. Itoh), gombos.zoltan@gmail.com (Z. Gombos).
[1] Present address: Genetic Research Center of Nagoya University, Furocyo, Chikusa, Nagoya 464-8602, Japan.

0005-2728/$ – see front matter © 2011 Elsevier B.V. All rights reserved.
doi:10.1016/j.bbabio.2011.10.002

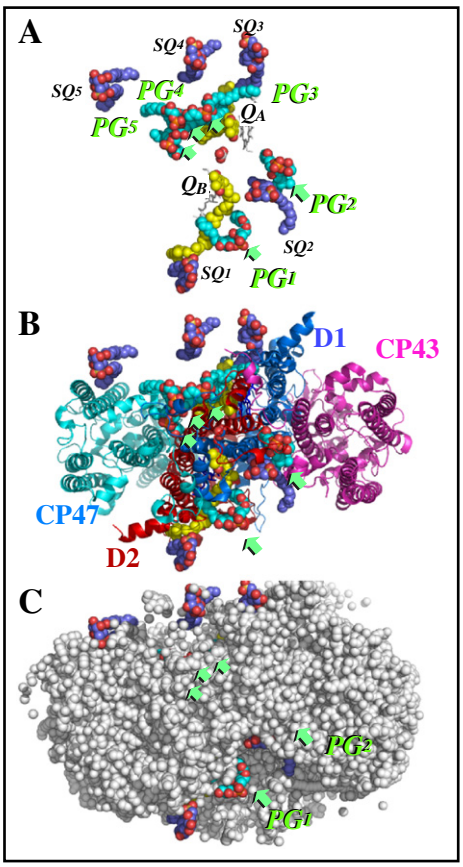

Fig. 1. Locations of negatively charged lipids, PG and SQDG (SQ), at the reducing-side surface of PS II RC monomer structure at 1.9 Å-resolution. A. Locations of cofactors. PG, SQDG and plastoquinone (Q_A and Q_B) are shown in space-filling models, and pheophytin *a* is shown as a stick model. Green arrows indicate the positions of head groups of PG. B. Locations of cofactors and protein subunits. Protein subunits, D1, D2, CP43 and CP47 are added to cofactors in A. C. A view of PSII surface on the reducing side. Cofactors and all the protein subunits including those in B are drawn in space filling models to show the exposure of lipids to the outer medium. Images were drawn with a MacPymol software and 3ARC.pdb data [12]. PG_{1-5} correspond to LHG:E772, D714, D702, L694 and D664, respectively. SQ_{1-5} correspond to SQDG:D768, A659, A667, L668, and B668, respectively, of 3ARC.pdb file.

shown in Fig. 1. Interestingly, the distributions of lipids are highly asymmetric. All the negatively charged lipids (SQDG and PG) are located on the reducing side surface of PSII as shown in Fig. 1 except for one MGDG at the periphery, and only the uncharged lipids are bound to the oxidizing side surface. It is, therefore, suggested that each PG molecule is specifically bound to a unique site on PSII and bears a specific functional/structural role together with the associated protein subunits. We attempted to identify the role of each PG identified on the structure in this study.

The role of lipids in photosynthesis has been studied either in *in vitro* extraction or after *in vivo* lipid degradation [1,13,14]. The treatment of thylakoid membranes with phospholipase C led to the suppression of PS II activity [13]. A specific role of PG in PS I was also suggested by Ikegami [15,16] who demonstrated that the addition of PG, but not that of MGDG, contributed to the reconstitution of chlorophylls (Chls) into ether-extracted PS I particles that are depleted of 95% of antenna Chls, two phylloquinones and most of lipids. The role of PG has been also studied *in vivo* in a mutant strain of *Synechocystis* sp. PCC6803 that has an inactivated gene encoding PG-phosphate synthase (pgsA) [3]. The *pgsA*-inactivated mutant strain produced by Hagio et al. [6] has been widely used to explore the role of PG. The mutant cells grew normally in media supplemented with PG, but showed suppressed oxygen-evolving activity with a concomitant decrease in Chl *a* and PG content [6]. Gombos et al. [5] have shown that the PG depletion induces the inactivation of the PS II secondary electron acceptor, plastoquinone Q_B. Sakurai et al. [7] pointed out that PG depletion leads to the destabilization of PS II dimers. Similar results were also reported by the inactivation of another gene *cdsA* that encodes cytidine 5′-diphosphate (CDP)-diacylglycerol synthase that is also required for PG synthesis [3,17]. PG was assumed to be important also for the formation of PS II dimer structure [7]. However, the 1.9 Å structure of PSII dimer crystal [12] does not contain PG at the binding surface of PSII monomers.

We studied oxygen evolution, Q_A to Q_B electron transfer reaction and fluorescence at 77 K to analyze the effects of depletion and re-addition of PG in the *ΔpgsA*- and *PAL/ΔcdsA*-mutant strains of *Synechocystis* sp. PCC6803. The results indicated two distinctly different PG functions in the regulation of Q_B together with the candidates of other PG action sites.

2. Materials and methods

2.1. Organisms and culture conditions

Cells of a Δ*pgsA* mutant strain [17] and a *PAL/ΔcdsA* strain [6] of *Synechocystis* sp. PCC6803 were grown photoautotrophically at 30 °C at a light intensity of 40 μmol m^{-2} s^{-1} in a BG11 medium supplemented with 5 mM HEPES-NaOH buffer (pH 7.5), 20 μg mL^{-1} kanamycin and 20 μmol dioleoyl-PG as described previously [4]. For the depletion of PG, cells grown in the PG-supplemented (+PG) medium were sedimented by centrifugation, washed twice with PG-free (−PG) culture medium, and then inoculated into the fresh PG-free medium. Wild-type cells were grown in the PG-free medium.

2.2. Measurement of absorption spectra and pigment concentration

Absorption spectra of cell suspensions were recorded with a wavelength resolution of 1 nm by a Shimadzu UV-1601 spectrophotometer in the cell chamber closer to a detector. Cell density was monitored by absorption at 720 nm that is mainly contributed by the light scattering of cells. Chl *a* concentration was calculated by the absorbance at 665 nm after the extraction of cells with 90% methanol with an extinction coefficient of 78.95 mM^{-1} cm^{-1} [18,19].

2.3. Electron microscopy

The harvested cells were fixed in 1% paraformaldehyde and 1% glutaraldehyde for 4 h at 4 °C and post-fixed in 1% osmium tetroxide. The samples were dehydrated in aqueous solutions of increasing ethanol concentrations, and then embedded in Spurr resin. Following polymerization, 85–90 nm ultra thin sections were cut out by a Reichert Ultracut E ultramicrotome. The sections were treated with uranyl acetate and lead citrate and subjected to electron microscopy in a Zeiss EM 902 electron microscope.

2.4. Measurements of oxygen evolution and fluorescence yield

Oxygen evolution was measured with a Clark-type electrode (Hanza Tec. Co.). The cells suspended in the growth medium inside a 1 cm-diameter tube were illuminated with white light from a halogen tungsten lamp through heat-cut filters at a nearly saturating intensity of 500 μmol photons m^{-2} s^{-1} as described previously [17].

Changes in the yield of chlorophyll fluorescence of cell suspension in a 10 mm light-path cuvette were monitored using a PAM fluorometer with a probing LED blue excitation flash, which was given at varied delay times with respect to the strong actinic excitation at a nearly saturating intensity with a red LED (Fl3000 Photon Systems Instruments, Kolackova, and Czech). Fluorescence yields

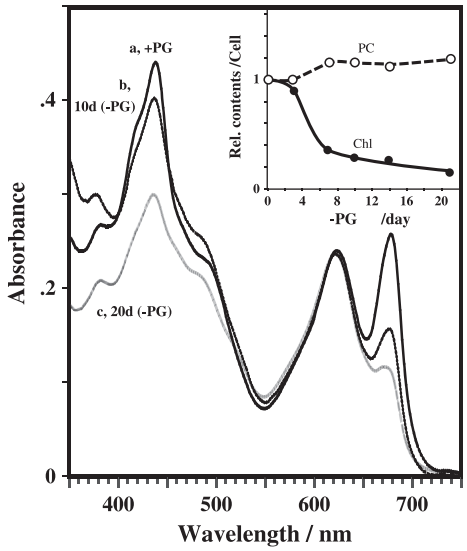

Fig. 2. Changes of absorption spectrum of *ΔpgsA* mutant cells cultured in −PG medium. a, b and c represent absorption spectra of cells cultured in −PG medium for 0 (+PG), 10 and 20 days, respectively. Each spectrum was corrected for the light scattering at 720 nm, and normalized at 620 nm peak of phycocyanin (PC). Inset. Changes of relative contents of PC and Chl *a* in cell. Peak heights of PC and Chl *a* bands with respect to absorbance at 720 nm of each cell suspension were calculated as rough measures of relative contents per cell. Effects of cell size changes to the 720 nm absorption/scattering were not considered.

were normalized as for the extent between the minimum (F_0) and maximum (F_M) yields measured before and just after the saturating excitation, respectively [22]. F_0 and F_M levels were almost unaffected by the moderate −PG treatment shorter than 10 days as shown in Fig. 5, although they were increased after 14 days of −PG treatment due to the higher fluorescence from allophycocyanin (APC) (see Fig. 8). F_M was, on the other hand, decreased by 5–30% on addition of BQ at 0.1–0.5 mM. These effects of long PG-depletion and high BQ concentrations were avoided in the measurements in Figs. 5 and 6 done at 0–7 d(−PG) treatments at 0–0.05 mM BQ.

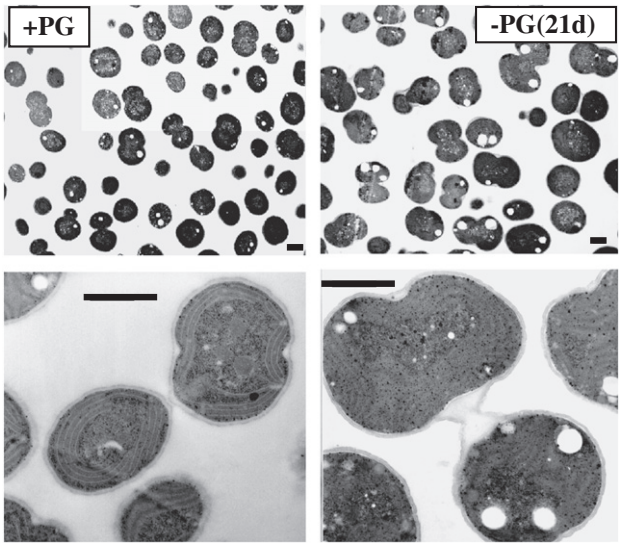

Fig. 3. Effects of PG depletion on the cell morphology of *ΔpgsA* cells. *Synechocystis* sp. PCC6803 *ΔpgsA* cells were cultured under +PG and 21 d(−PG) conditions, respectively. Upper and lower images show the images at different magnifications. A scale bar in each figure represents 1 μm. (Courtesy of Á. Párducz).

2.5. Measurements of fluorescence spectra and fluorescence lifetimes

Fluorescence spectra under continuous illumination were measured with a fluorescence spectrometer (F-3000, Hitachi, Hitachi, Japan) at 77 K with spectral resolution of 1.5 nm. Fluorescence emission spectra were not calibrated as for the detector sensitivity.

Simultaneous measurements of spectrum and picosecond decay kinetics of fluorescence at 77 K were done by using a streak camera system (Hamamatsu Photonics, Hamamatsu, Japan) in a single photon counting mode as described elsewhere [20,21]. Excitation light from a 405 nm diode laser, with a 60 ps duration and operated at 1 MHz repetition rate, was focused onto the sample cells (at a concentration of 40 μg Chl/ml) in a quartz cuvette (light path = 1 mm) placed in a cryostat (Oxford DN900, Oxford, UK) at 77 K. Fluorescence was dispersed in a 30 cm monochromator as for the emission wavelengths, and then, excited the photocathode of image intensifier. The electrons produced from the photocathode were accelerated inside the streak camera to give displacement as for the arriving times, excited the phosphor plate, and were detected by a CCD camera, and the traces of photons with intensities higher than the thermal noise level, were calculated. The system permitted the two-dimensional acquisition of fluorescence with respect to wavelength and time along the x and y axes, respectively, with wavelength resolution of 1 nm and the time resolution of 15 ps, respectively, under the present experimental condition (see Fig. SI1). We calculated the time-resolved spectra and the wavelength-resolved decay kinetics from the image as reported [21]. Fluorescence emission spectra were not calibrated as for the detector sensitivity.

3. Results

3.1. Effect of PG depletion on cell pigments

Fig. 2 shows the absorption spectra of Δ*pgsA* mutant cells of *Synechocystis* sp. PCC6803 [6] grown in a medium with (+PG) and without PG for 10 and 20 days, which are designated 10 d(−PG) and 20 d(−PG) cells hereafter, respectively. The absorbance at 720 nm was subtracted as the base line in Fig. 2. After normalization at the 620-nm peak of phycocyanin (PC) in phycobilisome (PBS), the Chl *a* bands were low in the PG-depleted cells. PC peak height normalized with respect to the cell turbidity, which was measured as the absorbance at 720 nm before the subtraction of baseline (inset in Fig. 2), was almost constant. The content of PC per cell, therefore, seems to be less affected as reported [4], although the turbidity may not be a precise measure of the cell number for the larger-PG cells (see Fig. 3). After 20 d(−PG) treatment, Chl *a* content was significantly lower than that of the +PG cells, while the PC content was similar (inset in Fig. 1), in line with the earlier observations [3–7]. PG depletion decreased the growth rate and the specific activity of oxygen evolution per Chl as shown in more detail below (see Fig. 4).

3.2. Effect of PG depletion on cell morphology

We studied the morphology of Δ*pgsA* mutant cells by negative-staining electron microscopy. Thin section of +PG cells (Fig. 3, +PG) showed round-shaped, normal-size *Synechocystis* cells with a small number of dividing cells (11 per 55 cells). The lower image in the expanded scale show cells with developed thylakoid membranes that sandwich densely-stained layers of phycobilisomes. Images of 21 d (−PG) cells (Fig. 3), on the other hand, showed larger cell sizes and most of them (25/30) are dividing incompletely. The dividing cells are even connected to another cell with transparent envelope suggesting the severe suppression of cell division process as shown in the lower panel. It seems that membrane formation itself is not suppressed much.

Both the +PG and −PG cells in Fig. 3 show the developed thylakoid membranes that are spaced at 50–60 nm each other

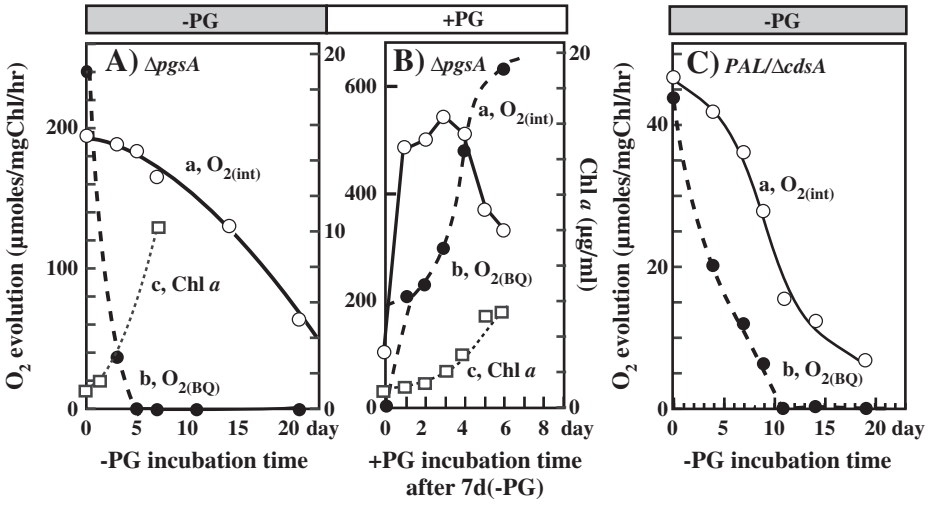

Fig. 4. Changes in the oxygen-evolving activities from H_2O to CO_2 (to the endogenous electron acceptors, $O_{2(int)}$), and H_2O to externally added BQ ($O_{2(BQ)}$) during PG depletion (−PG) and re-addition (+PG). A and B, activities during −PG treatment (A), and during PG re-addition after 7 d(−PG) treatment (B) in the Δ*pgsA* cells, respectively. C, activities during PG depletion in the *PAL*/Δ*cdsA* mutant cells. a and b represent oxygen evolution activities measured without ($O_{2(int)}$) and with BQ ($O_{2(BQ)}$), respectively. c, Chl *a* content in the growth medium.

sandwiching the dense granular layers of PBS. Therefore, the thylakoid membranes are formed even in the −PG cells probably due to the increase of other lipids that is known to compensate the PG loss [5–7]. Then, the thylakoid membranes in the −PG cell should contain comparable amount of PBS on the surface and much less amount of PSI, PSII and PG inside the membranes compared to those in the +PG cells.

3.3. Inhibition of the oxygen evolution and induction of the inhibition by p-benzoquinone by −PG treatment

The oxygen evolution activity driven by the illumination of red light at saturating intensity was measured during the PG depletion and re-addition in Δ*pgsA* cells (Fig. 4A and B). The +PG cells were once washed in the −PG medium and inoculated into the fresh −PG medium to start the PG-depletion culture. Two types of specific oxygen evolution activities per Chl amount were measured. The one, designated $O_{2(int)}$ hereafter, was measured in the absence of added artificial electron acceptors. The activity is supported by the intrinsic electron acceptors and CO_2 through PS I. The $O_{2(int)}$ was suppressed slowly to 70% after 6 days of −PG treatment under the present experimental condition (Fig. 4A). Longer PG depletion resulted in stronger suppression.

Chl content in the whole culture increased even in the −PG medium slowly (dotted lines with open squares in Fig. 4A), although the divisions of mutant cells are suppressed in the −PG medium as

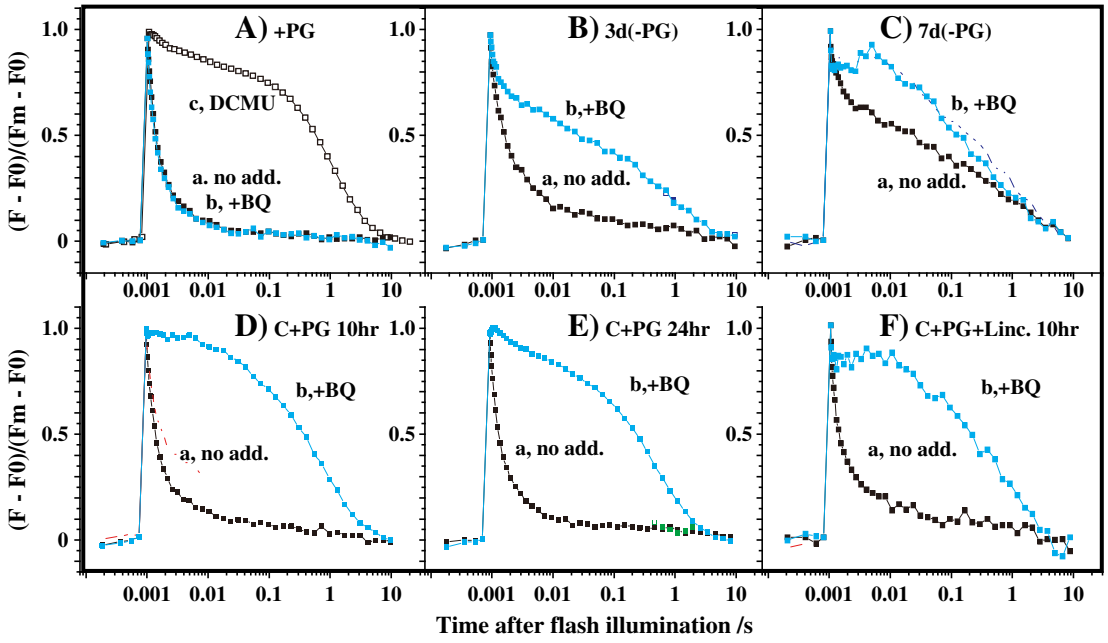

Fig. 5. Changes of flash-induced fluorescence yield induced by the strong actinic excitation, measured with a PAM fluorometer in Δ*pgsA* mutant cells. A, PG-supplemented cells (+PG). B and C, 3 d(−PG) and 7 d(−PG) cells, respectively. D and E, at 10 and 24 h, respectively, after re-addition of PG to 7 d(−PG) cells. F, at 10 h after re-addition of PG to 7 d(−PG) cells in the presence of lincomycin. a, b and c in A–F, correspond to no addition, +50 μM BQ, and +10 μM DCMU, respectively. BQ was added exactly at 1 min before each measurement.

seen in Fig. 3. Upon the inoculation into the +PG medium again after the 7 d(−PG) treatment, Chl content gradually increased (dotted lines with open squares in Fig. 4B) together with the re-start of cell division as reported [4–7,17].

We also measured the oxygen evolution activity supported by the added artificial electron acceptor, *p*-benzoquinone (BQ) and designated it as $O_{2(BQ)}$ hereafter. BQ is expected to accept electrons directly from PSII, from either Q_B or plastoquinone pool, by bypassing the PS I and cytochrome b_6/f complexes. In the +PG cells $O_{2(BQ)}$ was higher than $O_{2(int)}$ showing BQ to be an electron acceptor better than the intrinsic ones (broken lines and closed circles in Fig. 4A). However, $O_{2(BQ)}$ decreased rapidly after the start of PG depletion, and became null after 5 d(−PG) incubation. Surprisingly, the decrease occurred more rapidly than that of $O_{2(int)}$ that depends on both PSII and PSI activities. Therefore, BQ inhibits PS II activity only in the −PG cells, as do inhibitors like DCMU and atrazines that specifically inhibit the O_2 evolution in wild type cells by replacing plastoquinone in the Q_B binding site.

3.4. Effects of re-addition of PG

Re-addition of PG to the growth medium recovered the $O_{2(int)}$ and $O_{2(BQ)}$ activities from the low suppressed levels of the 7 d(−PG) cells (Fig. 4B). $O_{2(int)}$, which slowly decreased during the PG depletion, recovered very rapidly within a day after the re-addition of PG. On the other hand, $O_{2(BQ)}$, which decreased rapidly to zero during the 7 d (−PG) treatment, recovered more slowly after the re-addition of PG, showing a half recovery time of 4 days.

It can be summarized that $O_{2(int)}$ decreased slowly during the PG depletion and increased rapidly upon the PG re-addition. On the other hand, $O_{2(BQ)}$ decreased very rapidly during the PG depletion and increased very slowly upon the PG re-addition. These two types of activities responded to PG depletion differently, and suggest the existence of two different mechanisms or two different functional sites of PG. The recovery of cell growth, on the other hand, seems to occur more slowly after the re-addition of PG judging from the slow increase of Chl content in the growth medium (trace c in Fig. 4B).

The effects of PG depletion on $O_{2(int)}$ and $O_{2(BQ)}$ were also studied in *PAL*/Δ*cdsA*-mutant cells, which lack the *cdsA* gene and phycobilisomes [17]. The decrease of $O_{2(int)}$ occurred rapidly, and that of $O_{2(BQ)}$ (Fig. 4C) occurred slowly during the −PG treatment similar to those in Δ*pgsA*-mutant cells in Fig. 4A. Therefore, the two types of −PG effects on PSII are common in both types of mutant cells that lack different enzymes in the PG biosynthesis pathway [2,17]. The low $O_{2(int)}$ and $O_{2(BQ)}$ activities in the *PAL*/Δ*cdsA*-mutant cells seem to come from the absence of PSII antenna PC. We further studied the mechanisms of the two effects using Δ*pgsA*-mutant cells in the following sections.

3.5. Analysis of Q_A to Q_B electron transfer reaction monitored by flash-induced fluorescence yield

In order to see the exact target sites/mechanisms of PG depletion, we measured the flash-induced yield of fluorescence using a PAM fluorometer in Δ*pgsA* cells (Fig. 5). We monitored the fluorescence yield excited by a probing blue weak excitation flash to monitor the accumulation and dark decrease of Q_A^- after the illumination of the red actinic flash of saturating intensity. In the +PG cells, the high yield after the actinic flash decreased rapidly with an apparent time constant of 0.31 ms in the dark (Fig. 5A, curve a). The rise and decay indicate the photo-accumulation of Q_A^- and its dark oxidation by Q_B, respectively. The yield finally attained a lower level, which was determined by the equilibrium between electrons on Q_A^- and the pool plastoquinones [21].

The decay time courses of the fluorescence yield with and without BQ, which are hereafter designated $D_{(BQ)}$ and $D_{(int)}$, respectively, were almost the same each other in +PG cells (b and a in Fig. 5A). The results suggest that BQ does not oxidize Q_A^- directly, and acts as the electron acceptor to Q_B or pool plastoquinone under this condition. The addition of 10 μM DCMU, which is expected to bind at the Q_B site and to displace plastoquinone, eliminated the fast decay phase and increased the slow decay phase with an apparent time constant of about 0.9 s (open circles in Fig. 5A). The slow decay represents the charge recombination reaction between an electron on Q_A^- and a hole on the S_2 state in PS II [21].

We measured $D_{(int)}$ after various periods of PG depletion (Fig. 5A–C). The fast phase in $D_{(int)}$ was decreased by about 20% after 3 d(−PG) treatment (Fig. 5B). After 7 d(−PG) treatment, $D_{(int)}$ lost 60% of the fast phase (Fig. 5C). The slower decay phase at 0.01–10s was increased, indicating the suppression of electron transfer from Q_A^- to Q_B. The result indicates the requirement of PG for the proper function of Q_B.

Although $D_{(int)}$ in the 3 d(−PG) cells lost only 20% of the fast phase (Fig. 5B), $D_{(BQ)}$ lost more than 60% of the fast decay, suggesting the severer suppression of the Q_B function in the presence of BQ. This is rather strange because BQ is expected to serve as an external electron acceptor to Q_B or plastoquinone pool. In the 7 d(−PG) cells $D_{(int)}$ decreased its fast decay to 60% (Fig. 5C), while $D_{(BQ)}$ almost completely lost fast decay phase indicating the inactivation of Q_B, as does DCMU. The change of $D_{(BQ)}$, therefore, explains the suppression of $O_{2(BQ)}$ in Fig. 4 detected during the PG depletion. An apparent half time of the slow phase, which was enhanced by the addition of BQ, was calculated to be 0.4 s in each case in curve b in Fig. 5B–F and is shorter than that of 0.9 s measured in the presence of DCMU.

Fig. 5D–F represents the effects of re-addition of PG to 7 d(−PG) cells. Just 10 h after the re-addition of PG, $D_{(int)}$ fully recovered the fast phase (Fig. 5D). Similar rapid recovery was also seen in the presence of lincomycin (Fig. 5F), suggesting that the *de novo* synthesis of protein was not necessary for this recovery. On the other hand, we can still see the BQ effect on $D_{(BQ)}$ even at 1 day after the PG re-addition (Fig. 5E), at which time $D_{(int)}$ has already recovered the fast phase. It shows that the sensitivity of Q_B to BQ cannot be decreased within a short period even after addition of PG to the growth medium.

Fig. 6A plots amplitudes of the fast-decay phases in $D_{(int)}$ and $D_{(BQ)}$ against the lengths of PG depletion and PG re-addition, calculated from data as those in Fig. 5. Amplitude of the 0.3-ms decay phase

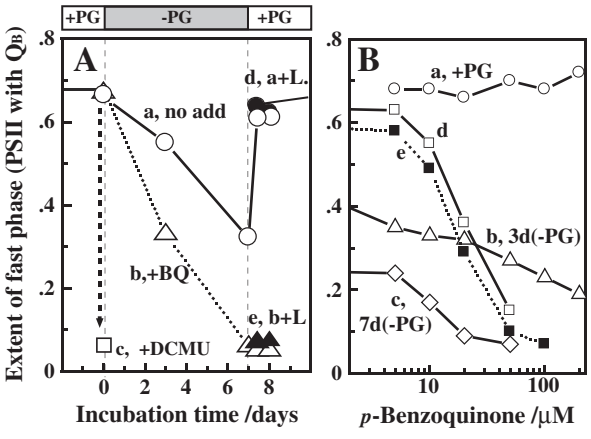

Fig. 6. A. Suppression and recovery of the fast decay phase of fluorescence during PG depletion and PG re-addition in the Δ*pgsA* mutant cells. a, b and c represent no addition, +50 μM BQ and +10 μM DCMU, respectively. In d and e, PG was re-added with lincomycin together with and without BQ, respectively. Relative amplitude of the fast phase (mainly the 0.3-ms decay phase with respect to the total extent of decay) was calculated as the difference between the extents at the initial peak (at 0 s) and at 1 ms after the peak from the results as those in Fig. 5. B. Dependence of the extent of the fast decay phase of fluorescence yield on the concentration of BQ during depletion and re-addition of PG in the Δ*pgsA* mutant cells. a, +PG cells. b, in 3 d(−PG) cells. c, in 7 d(−PG) cells. d, at 24 h after re-addition of PG to the 7 d(−PG) cells. e, similar to d, in the presence of lincomycin. BQ was added exactly at 1 min before each measurement.

was calculated as the extent of 0–1 ms decay. Relative extents of the fast phase in $D_{(int)}$ gradually decreased during PG depletion until the 7th day and was almost fully recovered already at 10 h after the re-addition of PG both in the presence and absence of lincomycin. On the other hand, the fast phase in $D_{(BQ)}$ disappeared faster than that in $D_{(int)}$, and it did not recover even at 1 day after the PG re-addition, at which time the fast phase in $D_{(int)}$ has been fully recovered. The two time courses are, thus, distinctly different. The time courses of inhibitions and recoveries of $O_{2(int)}$ and $O_{2(BQ)}$ in Fig. 4A resemble those of the fast phases in $D_{(int)}$ and $D_{(BQ)}$ in Fig. 6, respectively. Therefore, it is concluded that the modifications of the Q_B activity by PG and BQ induced the changes of $O_{2(int)}$ and $O_{2(BQ)}$ activities.

3.6. Modulation of affinity for BQ

We measured dependence of $D_{(BQ)}$ on the BQ concentration at different stages of −PG treatment, and plotted relative extents of fast phase (0–1 ms extent) against BQ concentration (Fig. 6B). In the +PG cells, the 2-min incubation with BQ had no effect at concentrations up to 0.2 mM BQ (trace a). The concentrations of BQ to suppress the fast phase to a half were 90 and 12 μM after 3 d (−PG) and 7 d (−PG) cells, respectively (curves b and c). After re-addition of PG, the high BQ sensitivity continued for a few days, giving half-maximum concentrations of around 20 μM both in the presence and absence of lincomycin (curves d and e, respectively). The results indicate that the PG depletion increased the affinity of BQ to the Q_B-inactivation site. The site seems to be newly created by the PG depletion. The high affinity of the site for BQ remained for a few days even after the full recovery of the Q_B activity ($D_{(int)}$) itself.

3.7. Effects of long-term incubation with BQ in the +PG and WT cells, and in spinach PS II

In the +PG cells, the fluorescence decay time course was not affected much even after 1-min incubation at 50 μM BQ (Fig. 7A). After 20 min incubation, we detected increase of the slow phase. In the WT cells, the 20-min incubation at 50 μM BQ did not affect the decay (Fig. 7B). The fast phase of $D_{(BQ)}$ was decreased by 30% after 40-min incubation at 500 μM BQ. The results in +PG and WT cells are in contrast to the 80% decrease detected in the 7 d(−PG) cells that was incubated at 50 μM BQ for 1 min in Fig. 5C. Therefore, BQ inhibits the Q_B reaction also in PS II in the +PG and WT cells very slowly. If we simply compare the times (1 min *vs.* 40 min) and effective concentrations of BQ (50 μM *vs.* 500 μM) between those in the +PG and 7 d(−PG) cells, the 7 d(−PG) treatment has increased the sensitivity to BQ more than 400 times.

We also tested the effect of BQ in the isolated spinach PS II particles (Fig. 7C). Even without BQ, the fluorescence decay was slow, probably due to the partial loss of plastoquinone from the Q_B site and the effect of detergent. The effect of 500 μM BQ after 40-min incubation on the fast phase was almost negligible, and the very slow decay phase at 0.1–10s was slightly accelerated. The results indicate the very low BQ sensitivity in the isolated spinach PS II particles.

3.8. Effects of PG-depletion on the fluorescence emission spectra at 77 K

We measured Chl fluorescence emission spectra at 77 K to study the functions and structures of PBS, PSI and PSII RCs under −PG conditions. Fig. 8A shows the fluorescence emission spectra measured with an excitation light at 430 nm that mainly excited Chl *a*. The +PG cells showed two PSII peaks at 684 and 695 nm and a high PSI

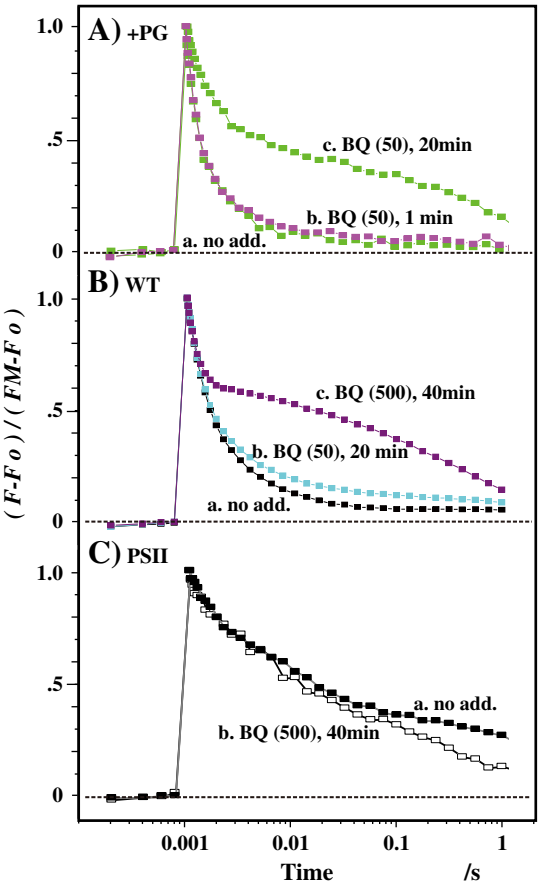

Fig. 7. Effects of long incubation at high concentrations of BQ on the fluorescence decay in the +PG Δ*pgsA* mutant cells (A), wild type cells (B) and spinach PS II particles (C). A, +PG cells. a, no addition. b and c, after 1 and 20 min incubation with 50 μM BQ. B, wild type cells. a, no addition. b, after 20 min incubation with 50 μM BQ. c, after 40 min incubation with 500 μM BQ. C, spinach PS II particles. a, no addition. b, after 40 min incubation with 500 μM BQ.

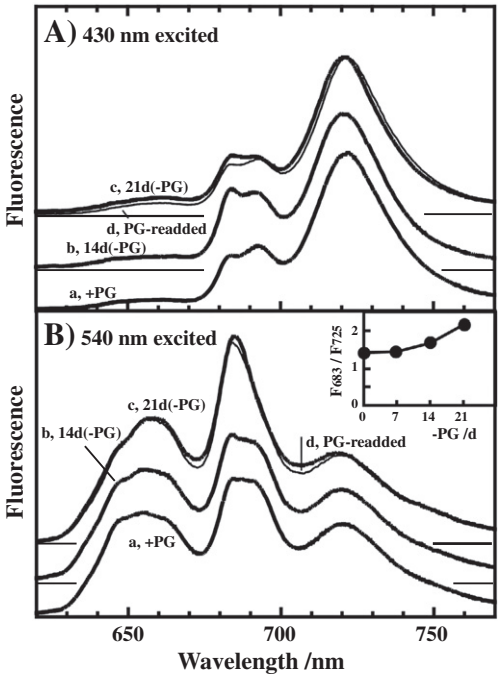

Fig. 8. Fluorescence emission spectra of Δ*pgsA* mutant cells at 77 K after varied lengths of PG depletion. A, excitation at 430 nm. B, excitation at 540 nm. a, b, c (thick lines) and d (thin line) represent +PG, 14 d(−PG), 21 d(−PG), and 1 d(+PG) treated after 21 d (−PG) treatment, respectively. Each spectrum was normalized at the PSI peak at around 720 nm. Base lines are shifted for each spectrum. Inset in B: ratio of the 683 nm peak height of PSII Chl fluorescence (F683) to the 725 nm peak height of PSI Chl fluorescence (F725) plotted against length of −PG treatment.

peak at 724 nm (trace a). Similar spectra were observed with 14 d (−PG) and 21 d(−PG) cells with a little higher peak at 684 nm after normalization at PSI peaks. Even in the 21 d (−PG) cells, PSII peaks were detected at 684 and 695 nm, together with the blue-shifted PSI peak at 718 nm. The blue shift of PSI peak seems to reflect the monomerization of PSI trimer induced by the depletion of PG [4]. Re-addition of PG to the 21 d(−PG) cells led to a slight decrease of the 684 nm peak and a 2-nm red shift of the 718 nm peak to give a spectrum similar to that in the +PG cells.

The results in Fig. 8A indicate that the PG depletion does not significantly modify the fluorescence spectrum and that Chls are properly organized in the PSI and PSII RCs even after the long −PG treatment. This indicates that there are almost no premature complexes that contain uncoupled Chls, which gave different emission spectra. Therefore, the −PG effects on the Q_B function is not associated with the significant structural change of PS II. This is rather unexpected because a partial loss (or weak binding) of CP43 from PSII RC was detected in the −PG cells in a *PAL/ΔcdsA* strain [17].

Fluorescence emission spectra were also measured with the excitation light at 540 nm that excited PC mainly (Fig. 8B). The +PG cells gave larger fluorescence peaks of PC at 655 nm and PSII-Chl *a* at 684 and 695 nm compared to those in the spectra excited at 430 nm, indicating the predominant energy transfer from PC to Chl *a* on PSII. In the 14 d(−PG) spectrum, the 684 nm band became a little larger. In the 21 d(−PG) spectrum the peak shifted to 682.5 nm and increased significantly. The PC band also became a little larger showing the high 655 nm peak. The large 682.5 nm band obscured the 695 nm band that is emitted from Chls on CP47 [23]. A 1-day incubation after re-addition of PG to the 21 d(−PG) cells induced a slight red shift of the PSI band with no effects on the positions and intensities of peaks of PSII Chls and PC (trace d in Fig. 8A and B). Inset figure shows the ratio of the 682–4 nm peak to PSI peak in the 540-nm-excited spectra. The ratio did not change until 7 d(−PG) treatment, and increased gradually after 14 days.

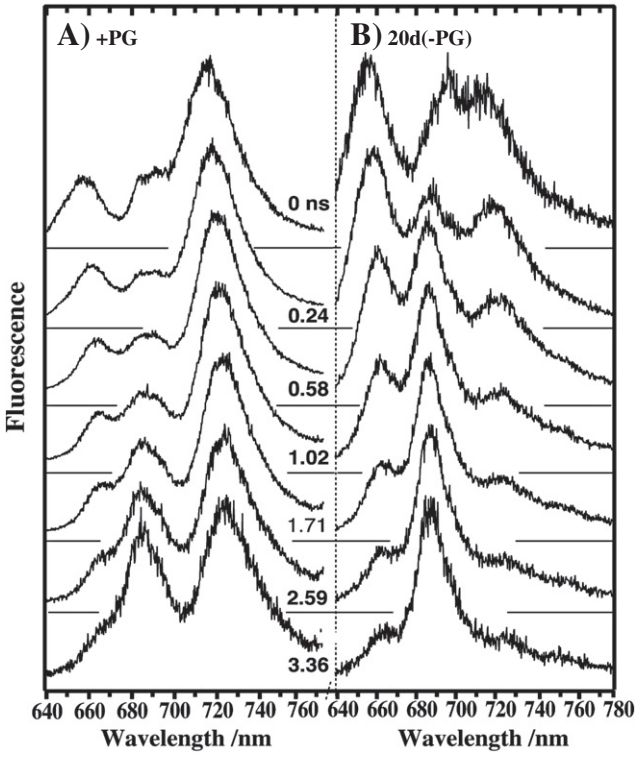

Fig. 9. Time-resolved fluorescence emission spectra at 77 K in Δ*pgsA* cells. A and B panels show the spectra from the +PG and 20 d(−PG) cells, respectively. Each spectrum was obtained as a slice for each 200 ps with a central decay time indicated in figure in ns, and normalized to the maximum peak. The data were obtained from the wavelength-decay 2-dimensional data as shown in Fig. SI1.

3.9. Effect of PG depletion on the fluorescence decay and the excitation energy transfer at 77 K

Simultaneous measurements of fluorescence decay and spectra were done at 77 K after the excitation with a 405-nm laser of 60-ps duration, which excited both PC and Chl *a*. Fluorescence intensities at different wavelengths and delay times were measured on the horizontal and vertical axes, respectively, as the 2D-images (see Fig. SI1). Each image covered a range at 640–780 nm and at 0–5 ns with respect to the laser peak. The images were very similar for the +PG, 7 d(−PG) and 14 d(−PG) cells, and somewhat different in the 20 d (−PG) cells. Therefore, it is concluded that the energy transfer process was not significantly affected by the PG-depletion shorter than 14 days, and was modified in the 20 d(−PG) cells.

Time-resolved fluorescence emission spectra of the +PG and 20 d (−PG) cells were calculated from the images in Fig. SI1 and shown in Fig. 9. Each spectrum was obtained as a slice for each 200 ps with a center decay time indicated in the figure and normalized to the maximum peak. In the +PG cells (Fig. 9A), fluorescence bands of PC at 660 nm, PSII Chl *a* at 684 and 694 nm, and PSI Chl *a* at 720 nm were detected. The PC band

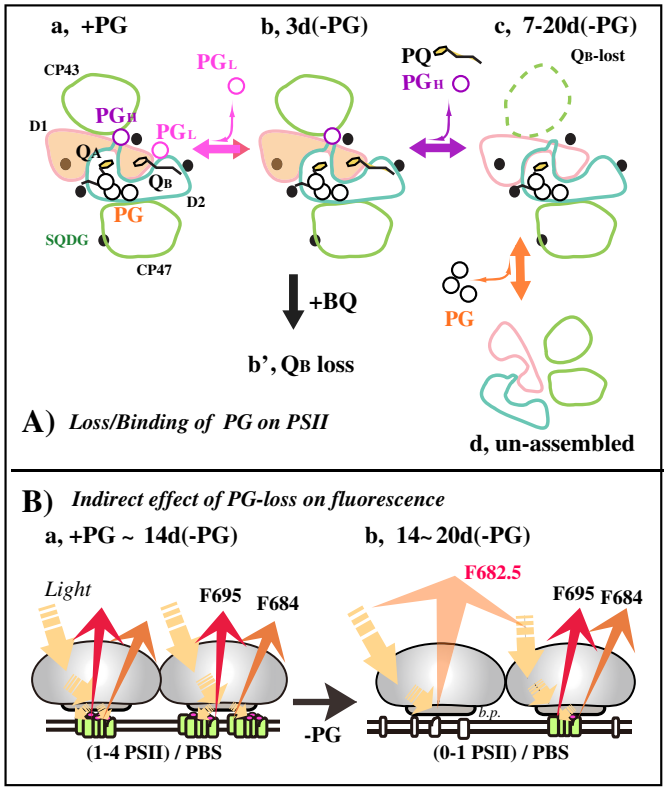

Fig. 10. A. A scheme for the loss/binding of PG on PSII during PG depletion/re-addition. States a, b, c, and d represent PSII states of +PG, 3 d(−PG), 7–20 d(−PG), and unassembled subunits, respectively. As the decrease of PG content, low affinity PG_L is lost from PSII first (state b) with still active Q_B. The loss of PG_L in state b allows the access of BQ that inactivates Q_B (state b′). Loss of high affinity PG_H from state b, then, destabilizes CP43 and D1, and leads to the loss of Q_B (state c). Further loss of tightly-bound PG from the Q_A side makes PSII to be decomposed into subunits (state d), and leads to the decrease of PSII content. We assume PG_H and PG_L to be PG_2 and PG_1, respectively, in PSII structure in Fig. 1. The scheme is also applicable to the PG-readdition process and the role of PG in the *de novo* synthesis/repair of PSII. B. Indirect effect of PG-depletion on the energy transfer from PBS to Chl. a, after 0–14 d (−PG) treatment. Energy transfer from PBS to PSII was not suppressed because of the flexible energy transfer mechanism. b, after 14–20 d (−PG) treatment. Some PBSs lack PSII and give 682.5 nm APC fluorescence at 77 K as seen in Figs. 8 and 9. See Discussion for more details.

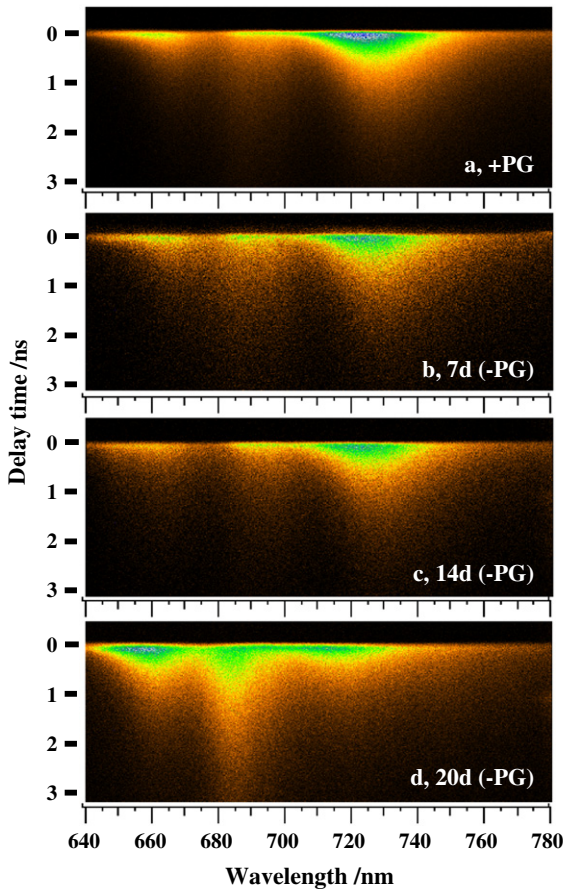

Fig. SI1. Wavelength-time 2-dimensional images of fluorescence decay induced by the 405 nm excitation laser flash at 77 K in Δ*pgsA* mutant cells of *Synechocystis* PCC 6803. From the top to the bottom: (+PG) cells, 7 d, 14 d and 20 d(−PG) cells. Fluorescence was excited by a 50 ps diode laser flash, which peak was set at time zero. Fluorescence emitted from the cell suspension was measured by a streak camera system as described in Materials and Methods. Each image shows the time after the laser peak along the vertical axis and the emission wavelength along the horizontal axis. Intensity of fluorescence increases in the order of blue, green, yellow, red and black colors.

at 660 nm was high at 0 ns, and then, decreased rapidly as seen at the longer delay times. The 684 and 695 nm bands were always detected at 0–1.02 ns. The peak around 684 nm lasted longer than the 660 nm PC band indicating the energy transfer from PC to PSII Chl. The PSI peak showed a red shift from 718 nm at 0 ns to 725 nm at 0.5 ns, and then decayed slowly. The PSI peak was the highest all the time. Similar results were obtained in the 7 d(−PG) and 14 d(−PG) cells (see Fig. SI1).

In the 20 d(−PG) spectrum, we observed a large PC peak at 655 nm at 0 ns (Fig. 9B). The peak decreased rapidly in almost parallel with the increase of the large 683 nm band, in a time range similar to that in the +PG cells. The 695-nm band at 0 ns was obscured by the overlapped large 683 nm band afterwards. PSI band gave a small peak at 718 nm at 0 ns and decayed almost similarly to that in the +PG cells. The spectrum at 3.36 ns showed only a huge 683 nm peak.

Apparent decay time constants were calculated by simulating the decay at each wavelength range (Table 1). Decay time constants (0.13, 0.53 and 1.3 ns) of PC at 663 nm in the 20 d(−PG) cells were almost similar to those (0.16, 0.53 and 1.1 ns) in the +PG cells. Time constants (0.077, 0.417 and 1.4 ns) of 684 nm band in the +PG cells were replaced apparently by a longer time constant (1.15 ns) in the 20 d(−PG) cells. PSI fluorescence became relatively smaller and exhibited a little longer time constant in the slower component (0.34 and 1.7 ns) in the 20 d(−PG) cells compared to those (0.37 and 1.1 ns) in the +PG cells, and gives a peak at 718 nm suggesting the modification of PSI trimer.

Table 1
Effects of PG depletion on the fluorescence decay kinetics at 77 K in the *Synechocystis* Δ*pgsA* mutant cells.

Cells	Center wavelength	$A_1(\tau_1)$	$A_2(\tau_2)$	$A_3(\tau_3)$
+PG	663 nm	0.50 (163 ps)	0.35 (525 ps)	0.15 (1080 ps)
	684 nm	0.63 (77 ps)	0.18 (417 ps)	0.19 (1440 ps)
	693 nm	0.65 (90 ps)	0.22 (466 ps)	0.13 (1550 ps)
	734 nm		0.60 (372 ps)	0.40 (1070 ps)
20 d(−PG)	663 nm	0.47 (125 ps)	0.44 (525 ps)	0.09 (1340 ps)
	684 nm		0.94 (1150 ps)	0.06 (4670 ps)
	693 nm	0.79 (71 ps)	0.12 (735 ps)	0.09 (1690 ps)
	734 nm		0.55 (339 ps)	0.45 (1690 ps)

Relative amplitude (A_i) of each fluorescence decay phase and decay time constant (τ_i) in parentheses was calculated at each emission range (with an indicated center wavelength ±2 nm) in Δ*pgsA* mutant cells. The cells were grown in the +PG medium or in the −PG medium for 20 days. A_i is expressed relatively as the initial intensity normalized for each wavelength range. τ_i was estimated by assuming the exponential decay of each component.

The results in Table 1 and Fig. 9 suggest that the large long-lifetime 683 nm peak in the 20 d(−PG) cells is emitted from APC that collects excitation energy from PC at the base plate of PBS and cannot transfer it to PSII.

4. Discussion

The results obtained in this study suggested multiple functional sites of PG in PSII. The *ΔpgsA* mutant cells in a −PG medium have been known to decrease oxygen evolution, amounts of Chl, PSII, PSI [2–7], PSI trimer [4], PS II dimer [7], and to inactivate Q_B [5]. PG was also shown to stabilize the CP43 binding to PS II in *PAL/ΔcdsA* mutant cells that lack PBS [17]. However, the relation between these effects and the exact locations of PG action sites has not been clear yet. We tried to discuss the relation between the multiple PG-depletion effects shown in this study and the PG locations reveled in the 1.9 A structure of *T. elongatus* PS II [12]. We first discuss about the two PG functional sites that regulate the Q_B function differently, mainly on the basis of effects of 0–10 d(−PG) treatments in Sections 4.1–4.7. Then, the mechanism of flexible energy transfer from PBS to PSII was discussed in Section 4.8, on the basis of detection of APC fluorescence only after the long 14–21 d(−PG) treatments.

4.1. Effects of PG depletion on the morphology and division of cell

PG is specifically required for the cell division of this organism because the large numbers of dividing cells were detected after the 20 d (−PG) treatment (Fig. 3). This confirms the conclusion in the *PAL/ΔcdsA* mutant cells that do not have PBS [17]. The result in Figs. 2 and 3 further indicated that PG-depletion did not suppress the formation of membranes and PBS. We can also assume almost constant PSI/PSII ratio during the PG depletion because the fluorescence spectra excited by Chl at 77 K (Fig. 8) was almost unchanged. The contents of Chl, PSII and PSI are significantly decreased in the 20 d(−PG) cells. Therefore, the thylakoid membranes should have high amount of PBS on the surface and significantly low amounts of PSII and PSI in its inside.

4.2. Two types of PG depletion effects on Q_B

The PG depletion induced two types of effects. The first type (designated L-type as interpreted below) increases the sensitivity to the inhibition by BQ because BQ addition suppressed the $O_{2(BQ)}$ and the fast 0.3 ms phase of $D_{(BQ)}$ in the early stage (3–5 days) of PG depletion. The second type (designated H-type) inhibits $O_{2(int)}$ and suppresses the fast phase of $D_{(int)}$ without BQ in the later stage (7–20 days) of PG-depletion. This effect was recovered rapidly within a day after the re-addition of PG.

The H-type effect corresponds to the gradual inhibition of O_2 evolution and Q_B activity reported [4–7,17]. On the other hand, the L-type

effect is identified firstly in this study. We confirmed similar phenomena in another *PAL*/Δ*cdsA* mutant cells (Fig. 3C) indicating that these effects were induced by the PG depletion itself.

4.3. Inactivation of Q_B by BQ after the short-term PG-depletion: L-type PG function

The $O_{2(BQ)}$ and the fast phase of $D_{(BQ)}$ were suppressed by BQ rapidly in the early stage of the PG depletion, and these effects were recovered very slowly over 5–10 days after PG re-addition. The parallelism indicates that BQ inactivates Q_B, and suppresses $O_{2(BQ)}$. BQ appears to work like a specific inhibitor of Q_B, as DCMU does, in the −PG cells. The effect is rather unexpected because BQ enhanced the oxygen evolution in the +PG cells as an artificial electron acceptor to Q_B. Therefore, it is suggested that Q_B in PSII RC is in a special condition that allows the inactivation by BQ after a short period of PG depletion. Apparent half times of the slow charge recombination in PSII were 0.4 s in the BQ-inactivated −PG cells and 0.9 s in the DCMU-inactivated +PG cells in Fig. 5. The result indicates that the binding of BQ to the Q_B site under −PG condition is a little different from that of DCMU. It is likely that the BQ-binding does not modify the redox potential of Q_A. Under this condition, PSII seems to be almost fully assembled as for proteins [17] and pigments as seen from the proper PSII fluorescence spectra and decays (Figs. 8 and 9).

It is assumed that the short-term −PG treatment depleted PG from its functional site, at which PG guards Q_B from the BQ-effect. The affinity of BQ to its Q_B-inactivating site (in the vicinity of Q_B or in the Q_B site itself) was increased more than 400 times to give a low dissociation constant of 12–20 μM in the PG-depleted cells (Fig. 6B).

4.4. Inactivation of Q_B (without BQ) after the long-term PG depletion; H-type PG function

$O_{2(int)}$ and the fast phase of $D_{(int)}$ were decreased slowly during the long-term PG-depletion over 10 days, and were rapidly recovered within 10 h after the inoculation into the +PG medium (H-type effects). The rapid recovery was not affected by lincomycin, indicating no requirement for the *de novo* synthesis of proteins.

The slow inactivation of Q_B (without BQ) confirms the previous reports of the thermoluminescence, PAM, and fluorescence decay results in the Δ*pgsA* [5] or *PAL*/Δ*cdsA* cells [17]. After the long −PG treatments, mutant cells showed no $S_2Q_B^-$ band and showed only the $S_2Q_A^-$ band of thermoluminescence suggesting the inhibition of electron transfer from Q_A^- to Q_B [5]. This $S_2Q_A^-$ peak was shifted by DCMU indicating that DCMU binds to the remaining Q_B site and shifts the Q_A redox potential [5]. Therefore, the Q_B site seems to be modified by the long PG loss to decrease the affinity to plastoquinone, although the site still can bind DCMU. The results of BN-PAGE [17] also indicated the partial dissociation of CP43 from the PS II complex after the PG depletion. On the other hand, the inactivated Q_B function was rapidly recovered by the PG re-addition even in the presence of lincomycin within 10 h. Therefore, the mechanism for the H-type effect may occur by the modification of the Q_B site to decrease the affinities of plastoquinone and CP43.

4.5. Low- and high-affinity PG action sites: PG_L and PG_H

We named two types of PG effects as L- and H-types based on the affinity difference as discussed below. The recovery from the H-type effect occurred rapidly in the presence of lincomycin and does not seem to be coupled to the protein synthesis/degradation. The recovery from the L-type effect, on the other hand, occurred after a long delay of 3–7 days. The two effects, therefore, behaved rather independently, although they might be coupled somehow. It is clear that both effects are regulated by the PG contents in the cells.

We propose an "affinity mechanism", which assumes the high- and low-affinity PG-action sites (designated PG_H and PG_L sites, respectively) for the H- and L-type effects. In general, all the PG-binding sites in each cell must have been filled with PG during the +PG growth, and newly synthesized PG will be supplied to new fractions of membranes and complexes. Upon the transfer into the −PG medium, the low affinity PG_L sites will loose PG faster than that on the high affinity PG_H sites in response to the gradual change of PG concentration inside cells. On the other hand, after the long-term PG depletion the recovery of PG to the PG_L sites will be delayed because it will be accomplished only after the full binding of PG to the high-PG-affinity sites including the PG_H sites.

The "affinity mechanism", then, explains the L-type effect to be caused by the fast-depletion/slow-recovery of PG (PG_L) at the low-affinity site. We can assume that the rapid loss of PG_L makes the Q_B function sensitive to the BQ inhibition, and that PG_L will be only slowly regained after the start of PG re-addition. On the other hand, the slow suppression and the rapid recovery of the H-type effect can be explained by the slow-depletion/fast-recovery of PG (PG_H) at the high-affinity site. The "affinity mechanism", thus, explains the L- and H-type effects well. Even if PG_L and PG_H interact somehow each other, or their bindings are coupled "in a series", their bindings will still be regulated by the affinity difference.

4.6. Molecular mechanisms of the functions of PG_H and PG_L

The depletion of PG from the growth medium of Δ*pgsA* or *PAL*/Δ*cdsA* cells has been known to suppress oxygen evolution activity ($O_{2(int)}$) [3,5,6,17] and the electron transfer from Q_A to Q_B [5], and to increase PSII with weakly-bound CP43 [17]. These effects occurred in a time range similar to that for the H-type effects. Therefore, we can assume that PG_H works for the tight binding of CP43 and for the proper configuration of D1 subunit that is required for the function/binding of Q_B.

The results in the present study indicated that depletion of PG_L triggers the BQ-induced inhibition (L-type effect). The release of PG_L seems to increase the accessibility of BQ to the target site in the vicinity of Q_B because the −PG treatment decreased the BQ concentrations required for the Q_B inactivation (Fig. 6B), and increased the BQ sensitivity more than 400 times (Fig. 7A). Another possible mechanism may be that the PG-depletion increased the permeability of cell membranes to BQ and increased the BQ concentration inside cells. However, this seems to be unrealistic because BQ enhanced the rate of oxygen evolution as the efficient electron acceptor in the +PG cells, and did not suppress the Q_B activity in the isolated spinach PS II. We, therefore, assume that PG_L functions like a gatekeeper against the access of BQ (or its semiquinone form), which inactivates Q_B function probably by binding to the Q_B site or/and displacing plastoquinone. The BQ binding is greatly enhanced by the loss of PG_L. The role of PG_L, which protects Q_B from the attack by BQ, is indicated for the first time. Similar effect was detected with dichrolo-*p*-benzoquinone in our preliminary study. Studies with variety of quinone species will help understanding of the mechanism of L-type effect.

4.7. Locations of PG_H and PG_L in PSII structure

In the five PG molecules identified in the 1.9 Å structure of PS II of *T. elongatus* [12] (Fig. 1), two are located nearby Q_B. They form a lose cluster with two SQDG (PG_2-SQ_2-PG_1-SQ_1) on the lumenal surface. Polar head groups of the latter three are exposed to the medium partially (Fig. 1C), while PG_2 is fully covered by a loop from D2, and in contact with CP43 and D1 subunits. PG_2, therefore, seems to be tightly bound to PSII, acting like an anchor bolt for the assembly of the three subunits [10,12]. The loss of PG_2 will affect the structures/bindings of these subunits, and also may affect the structure of Q_B site that is situated on the other side of a membrane-spanning helix of D1 from

PG_2. On the other hand, PG_1 is in contact with the Q_B tail and is not in contact with CP43 [10,12]. PG_1, which is sandwiched by SQ_1 and SQ_2, was once estimated to form the plastoquinone path [10]. We can also assume PG_1 to be more weakly bound to PS II compared to PG_2 based on their different temperature factors [12].

PG_H and PG_L may be either, 1) PG_2 and PG_1, 2) PG_1 and another PG, or 3) PG molecules other than PG_2 and PG_1, respectively. The case 1 interprets the high and low affinities of PG_H and PG_L well, with the different locations of PG_2 and PG_1. Fig. 10A represents a current model of the PG depletion/recovery process by assuming case 1. PG_1 is distant from D2 and CP43, and is exposed to the outer medium. If PG_1 is lost or replaced (b state), we will not see a big change of PSII structure except a hall on the surface connected to Q_B tail. Such a hall will weaken the affinity of Q_B binding and increase the accessibility of small molecules like BQ in the outer medium to the Q_B site to displace or inactivate Q_B (b′ state). On the other hand, the loss of PG_2, or replacement by another lipid, will significantly weaken the binding of CP43, and may affect the D1 and D2 structures to displace Q_B even without BQ (c state). The other three PG_{3-5} molecules located nearby Q_A site do not seem to be depleted easily because we did not detect changes in the Q_A function during the −PG treatment. Their loss seems to occur only after the loss of PG_1 and PG_2. The loss may result in the destruction of whole PSII structure (d state) because it will also detach CP47 from PSII. We, thus, conclude that case 1 shown in Fig. 10A is a best working hypothesis at present, although it is difficult to fully deny the other possibilities.

4.8. Pigment system and PSII structure in the −PG cells

The PG depletion decreased Chl content of the cells suggesting the PG requirement for the assemblies of PSI and PSII. As for PSI, PG-depletion suppressed the trimer formation and significantly decreased the PSI content [4]. It may come from the requirement of PG molecules, which are tightly bound inside PSI, for the assembly of PSI. The protein analysis also showed the decrease of PSI and PSII contents [17].

The 10 d(−PG) and 20 d(−PG) treatments decreased the Chl content to almost 25 and 18%, respectively, with respect to the cell turbidity with almost constant PBS contents (Fig. 2). This situation seems to have produced anomalously high PBS/PSII ratios. Although the 21 d(−PG) cells showed the fluorescence spectrum with increased APC fluorescence at 683 nm at 77 K when excited at the PC absorption band, the emission spectrum excited at the 430-nm Chl band was not modified much. Therefore, assemblies of Chl and proteins on the PSII seem to be accomplished almost normally even in the 20 d(−PG) cells. The assemblies of Chl *a* on the PSI monomer complex also seemed to be normal because we detected a rapid rise of the 723-nm PSI fluorescence band that indicates the fast energy transfer from the shorter-wavelength antenna Chls on PSI. The shift of 725-nm peak to 723 m suggests the decrease of PSI trimer in the 20 d(−PG) cells as reported [4].

The defect in the energy transfer from PBS to PSII was detected only in the 20–21 d(−PG) cells as the increase of 682.5 nm fluorescence band with a long 1.15 ns lifetime from APC. However, the PG depletion caused almost no effects on the fluorescence of PBS and RC as far as Chl content is higher than 25%. PG, therefore, is not required for the contact of PBS to membrane and to PSII, for the synthesis and assembly of PBS, and for the energy transfer from PC to APC inside PBS. The energy transfer from PBS to PSII, therefore, seems to be very flexible and independent of PG. One phycobilisome seems to give the excitation energy to variable numbers of PSII at PSII/PBS ratios of 1–4 if we assume the PSII/PBS ratio of 1 to be the lower limit as schematically shown in Fig. 10B. Single PBS, therefore, is estimated to give the excitation energy to nearly two dimers (4 PSII RC) and to less than one monomer of PSII in the +PG and 20 d(−PG) cells, respectively. Some PBS may transfer energy also to PSI even in the −PG cells because we detected almost constant ratio of PSII/PSI in the 77 K emission spectra. The results suggest that PG is indispensable for the stabilization of PSI and PSII RCs, and that some amounts of RCs, which are almost mature as for pigment system, can be formed even under the severe PG depletion.

5. Conclusion

The results in the present study indicated that two PG molecules regulate the Q_B function differently as shown in Fig. 10A. PG is also required for the assembly/stabilization of both PSII and PSI. PG is also shown to be required for the cell division specifically. On the other hand, PG is not required for the formation, binding to membranes and energy transfer of PBS. PBS-PSII (or PSI) interaction seems to be very flexible and is not affected by the PG depletion directly as shown in Fig. 10B. As shown in previous study [17] *de novo* synthesis of PSI and PSII protein subunits are not suppressed, while the assemblies into the mature PSI and PSII complexes seem to require PG. Present study also showed that PBS formation and its attachment to the membranes are not affected by PG.

We identified a low-affinity PG (PG_L), which guards Q_B from the attack of BQ that inactivates Q_B. We assume PG_L to correspond to PG_1 shown in the PSII structure in Fig. 1. On the other hand, PG_H is required to bind CP43 and Q_B. The loss of PG_H is estimated to modify the structure of D1 protein and release Q_B [5,17]. We assume PG_H to correspond to PG_2. A cluster of the other three PG_{3-5} molecules around Q_A that are very tightly bound to PSII shown in Fig. 1, may be essential for the assembly of D2 and whole PSII. Thus, PSII may not be formed properly without PG_{3-5}. A scheme in Fig. 10 interprets the PG-depletion process and also seems to interpret the repair or *de novo* assembly process of PSII. Negative lipids nearby phylloquinones in PSI [8] might function like PG_{3-5} in PSII. On the other hand, it remains to be studied whether PG also functions in the sites other than PSII to affect the long path electron transfer or not. It is interesting that each PG molecule in PSII seems to have its specific role in the regulation of cofactor functions, in addition to its structural role to simply fill the space.

Acknowledgment

We thank Dr. H. Wada of Tokyo Univ. for his kind gift of a Δ*pgsA*-mutant strain of *Synechocystis* sp. PCC6803 to Z. G. and his valuable discussions during the study. We also thank Drs Y. Shibata, H. Mino, Y. Nakamura and K. Maki in Division of Material Science, Physics, in Nagoya Univ. S. I. thanks Dr. M. Ishiura in Genetic Research Center of Nagoya Univ. for his support for the work. The work was financially supported by a Grant-in-Aid for Scientific Research from the Japanese Ministry of Education, Culture, Sports, Science, and Technology to S. I. and by the Hungarian Science Foundation to Z.G. (OTKA: grants K 60109, K 68692, and K 82052).

References

[1] N. Murata, P.-A. Siegenthaler, Lipids in photosynthesis: an overview, Lipids in photosynthesis: structure, function and genetics, in: P.-A. Siegenthaler, N. Murata (Eds.), Advances in Photosynthesis, vol. 6, Kluwer Academic Publishers, Dordrecht, The Netherlands, 1998, pp. 1–20.
[2] M. Hagio, I. Sakurai, S. Sato, T. Kato, S. Tabata, H. Wada, Phosphatidylglycerol is essential for the development of thylakoid membranes in *Arabidopsis thaliana*, Plant Cell Physiol. 43 (2002) 1456.
[3] N. Sato, M. Hagio, H. Wada, M. Tsuzuki, Requirement of phosphatidylglycerol for photosynthetic function in thylakoid membranes, Proc. Natl. Acad. Sci. U. S. A. 97 (2000) 10655.
[4] I. Domonkos, P. Malec, A. Sallai, L. Kovacs, K. Itoh, G.Z. Shen, B. Ughy, B. Bogos, I. Sakurai, M. Kis, K. Strzalka, H. Wada, S. Itoh, T. Farkas, Z. Gombos, Phosphatidylglycerol is essential for oligomerization of photosystem I reaction center, Plant Physiol. 134 (2004) 1471.
[5] Z. Gombos, Z. Varkonyi, M. Hagio, M. Iwaki, L. Kovacs, K. Masamoto, S. Itoh, H. Wada, Phosphatidylglycerol requirement for the function of electron acceptor plastoquinone Q(B) in the photosystem II reaction center, Biochemistry 41 (2002) 3796.

[6] M. Hagio, Z. Gombos, Z. Varkonyi, K. Masamoto, N. Sato, M. Tsuzuki, H. Wada, Direct evidence for requirement of phosphatidylglycerol in photosystem II of photosynthesis, Plant Physiol. 124 (2000) 795.
[7] I. Sakurai, M. Hagio, Z. Gombos, T. Tyystjarvi, V. Paakkarinen, E.M. Aro, H. Wada, Requirement of phosphatidylglycerol for maintenance of photosynthetic machinery, Plant Physiol. 133 (2003) 1376.
[8] P. Jordan, P. Fromme, H.T. Witt, O. Klukas, W. Saenger, N. Krauss, Three-dimensional structure of cyanobacterial photosystem I at 2.5 angstrom resolution, Nature 411 (2001) 909.
[9] B. Loll, J. Kern, W. Saenger, A. Zouni, J. Biesiadka, Towards complete cofactor arrangement in the 3.0 A resolution structure of photosystem II, Nature 438 (2005) 1040.
[10] A. Guskov, J. Kern, A. Gabdulkhakov, M. Broser, A. Zouni, W. Saenger, Cyanobacterial photosystem II at 2.9-Å resolution and the role of quinones, lipids, channels and chloride, Nat. Struct. Mol. Biol. 16 (2009) 334.
[11] I. Sakurai, J.R. Shen, J. Leng, S. Ohashi, M. Kobayashi, H. Wada, Lipids in oxygen-evolving photosystem II complexes of cyanobacteria and higher plants, J. Biochem. 140 (2006) 201.
[12] Y. Umena, K. Kawakami, J.-R. Shen, N. Kamiya, Crystal structure of oxygen-evolving photosystem II at a resolution of 1.9 Å, Nature 473 (2011) 55.
[13] M. Droppa, G. Horváth, E. Hideg, T. Farkas, The role of phospholipids in regulating photosynthetic electron transport activities: treatment of thylakoids with phospholipase C, Photosynth. Res. 46 (1995) 287.
[14] B. Essigmann, S. Guler, R.A. Narang, D. Linke, C. Benning, Phosphate availability affects the thylakoid lipid composition and the expression of SQD1, a gene required for sulfolipid biosynthesis in *Arabidopsis thaliana*, Proc. Natl. Acad. Sci. U. S. A. 95 (1998) 1950.
[15] I. Ikegami, Reconstitution of antenna chlorophyll-a in spinach PSI complex, Photosynth. Res. 34 (1992) 131.
[16] I. Ikegami, S. Itoh, M. Iwaki, Selective extraction of antenna chlorophylls, carotenoids and quinones from photosystem I reaction center, Plant Cell Physiol. 41 (2000) 1085.
[17] H. Laczko-Dobos, B. Ughy, S.Z. Toth, J. Kornenda, O. Zsiros, I. Domonkos, A. Parducz, B. Bogos, M. Komura, S. Itoh, Z. Gombos, Role of phosphatidylglycerol in the function and assembly of Photosystem II reaction center, studied in a *cdsA*-inactivated PAL mutant strain of *Synechocystis sp.* PCC6803 that lacks phycobilisomes, Biochim. Biophys. Acta 1777 (2008) 1184.
[18] M.M. Allen, Simple conditions for growth of unicellular blue-green algae on plates, J. Phycol. 4 (1968) 1.
[19] H.K. Lichtenthaler, Chlorophylls and carotenoids: pigments of photosynthetic biomembranes, Methods Enzymol. 148 (1987) 350.
[20] A.M. Gilmore, S. Matsubara, M.C. Ball, D.H. Barker, S. Itoh, Excitation energy flow at 77 K in the photosynthetic apparatus of overwintering evergreens, Plant Cell Environ. 26 (2003) 1021.
[21] M. Komura, Y. Shibata, S. Itoh, A new fluorescence band F689 in photosystem II revealed by picosecond analysis at 4–77 K: function of two terminal energy sinks F689 and F695 in PS II, Biochim. Biophys. Acta 1757 (2006) 1657.
[22] U. Schreiber, C. Neubauer, U. Schliwa, Pam fluorometer based on medium-frequency pulsed Xe-flash measuring light — a highly sensitive new tool in basic and applied photosynthesis research, Photosynth. Res. 36 (1993) 65.
[23] E.G. Andrizhiyevskaya, D. Frolov, R. van Grondelle, J.P. Dekker, On the role of the CP47 core antenna in the energy transfer and trapping dynamics of Photosystem II, Phys. Chem. Chem. Phys. 6 (2004) 4810.